Conjugation of a Magainin Analogue with Lipophilic Acids Controls Hydrophobicity, Solution Assembly, and Cell Selectivity

Dorit Avrahami and Yechiel Shai*

Department of Biological Chemistry, Weizmann Institute of Science, Rehovot, 76100 Israel

Received July 24, 2001; Revised Manuscript Received November 15, 2001

ABSTRACT: Our basic understanding of how to combat fungal infections has not kept pace with the recent sharp rise in life-threatening cases found particularly among immuno-compromised individuals. Current investigations for new potential antifungal agents have focused on antimicrobial peptides, which are used as a cell-free defense mechanism in all organisms. Unfortunately, despite their high antibacterial activity, most of them are not active toward fungi, the reason of which is not clear. Here, we present a new approach to modify an antibacterial peptide, a magainin analogue, to display antifungal activity by its conjugation with lipophilic acids. This approach has the advantage of producing well-defined changes in hydrophobicity, secondary structure, and self-association. These modifications were characterized in solution at physiological concentrations using CD spectroscopy, tryptophan fluorescence, and analytical ultracentrifugation. In order of increasing hydrophobicity, the attachment to the magainin-2 analogue of (i) heptanoic acid results in a monomeric, unordered structure, (ii) undecanoic acid yields concentration-dependent oligomers of α helices, and (iii) palmitic acid yields concentration-independent α-helical monomers, a novel lipopeptide structure, which is resistant to proteolytic digestion. Membrane−lipopeptide interactions and the membrane-bound structures were studied using fluorescence and ATR-FTIR in PC/PE/PI/ergosterol (5/2.5/2.5/1, w/w) SUV, which constitute the major components of *Candida albicans* bilayers. A direct correlation was found between oligomerization of the lipopeptides in solution and potent antifungal activity. These results provide insight to a new approach of modulating hydrophobicity and self-assembly of antimicrobial peptides in solution, without altering the sequence of the peptidic chain. These studies also provide a general means of developing a new group of lipopeptide candidates as therapeutic agents against fungal infections.

The number of life-threatening fungal infections has increased sharply in recent years because of the growing number of immuno-compromised individuals and the emergence of increasing numbers of isolates resistant to the few effective antifungal agents available (*1*, *2*). Studies on antifungal drugs have generally lagged behind those on antibiotics, mainly because fungal and mammalian cells are both eukaryotic, making differential selectivity in targets more difficult. Current investigations for new potential antifungal agents have focused on antimicrobial peptides, which are used as a cell-free defense mechanism in all organisms. In higher organisms, it complements the highly specific cell-mediated immune response (*3*, *4*). Most antimicrobial peptides are highly active toward bacteria; however, some are also active toward fungi (*5*, *6*). The most studied group within this antimicrobial peptides contains short, linear, positively charged, amphipathic peptides, whose activities and possible modes of action have been reviewed in detail (*7*−*12*). It is believed that most antimicrobial peptides target the negatively charged outer leaflet membrane of bacteria directly, rather than acting via a specific receptor. This has been demonstrated by the findings that antimicrobial peptide chirality is not important for activity (*13*−*15*) and that most native antimicrobial peptides preferentially permeate negatively charged model phospholipid membranes, which mimic bacterial membrane composition. The low affinity of most antimicrobial peptides for zwitterionic membranes, mimicking eukaryotic cell outer membranes (*16*), explains their inability to lyse erythrocytes and fungi.

A few native positively charged antimicrobial peptides, such as dermaseptins, pardaxin analogues, and the human-like cecropin, LL-37 (*17*−*19*), are both antibacterial and antifungal. They bind and permeate efficiently both zwitterionic and negatively charged phospholipid vesicles. Studies of their modes of action indicate that they self-associate in solution and in membranes. Self-association is driven either by a hydrophobic N- or C-terminus or by specific amino acids in the peptide sequence, resulting in the formation of α-helical bundles that could initiate strong hydrophobic binding to zwitterionic membranes (*17*−*19*). Moreover, these studies suggest that mutations, which increase the hydrophobicity of positively charged antimicrobial peptides caus-

* The Harold S. and Harriet B. Brady Professorial Chair in Cancer Research. To whom correspondence should be addressed. Phone: 972-8-9342711. Fax: 972-8-9344112. E-mail: Yechiel.Shai@weizmann.ac.il.

10.1021/bi011549t CCC: $22.00
Published on Web 01/26/2002

ing them to assemble in solution and in membranes, should make them antifungal. However, such mutations can affect other intrinsic properties of the peptides, such as secondary structure and amphipathicity, which also influence biological function. In this study, we utilized a new approach to increase peptide hydrophobicity and ability to self-associate, without altering the properties of the peptidic chain. More specifically, we attached lipophilic acids of different lengths to the N-terminus of magainin, a well-characterized, α-helical, positively charged, nonhemolytic antibacterial peptide. Its poor antifungal activity is an advantage, allowing us to measure and correlate the effects of lipophilic acid attachment to biological activity with oligomeric state and to model membrane interactions. Previous studies reported that magainin adopts a monomeric unordered structure in aqueous solution and a highly α-helical structure upon membrane binding (*20*). Here, the attachment of heptanoic, undecanoic, and palmitic acids to the N-terminus of a magainin analogue results in lipopeptides with three distinct structures and oligomeric states in solution, at the minimal inhibitory concentration (MIC) as revealed by fluorescence, CD[1] spectroscopies, and analytical ultracentrifugation. ATR-FTIR and fluorescence spectroscopy were used to investigate the membrane-bound lipopeptides. The resulting trends are discussed, focusing in particular on the mode of action of this group of lipopeptides and their requirements for inducing antifungal activity.

MATERIALS AND METHODS

Materials. Rink amide MBHA resin, 4-methyl benzhydrylamine resin (BHA), and 9-fluorenylmethoxycarbonyl (F-moc) amino acids were obtained from Calbiochem-Novabiochem AG (Switzerland). Other reagents used for peptide synthesis included trifluoroacetic acid (TFA; Sigma, St. Louis, MO), piperidine (Merck, Whitehouse Station, NJ), *N*,*N*-diisopropylethylamine (DIEA; Sigma), *N*-hydroxybenzotriazole hydrate (HOBT; Aldrich, St. Louis, MO), 2-(1*H*-benzotriazole-1-yl)-1,1,3,3-tetramethyluronium hexafluorophosphate (HBTU), and dimethylformamide (DMF, peptide synthesis grade; Biolab Jerusalem, Israel). Egg phosphatidylcholine (PC), phosphatidylinositol (PI), and phosphatidylethanolamine (PE) ergosterol were purchased from Lipid Products (South Nutfield, U.K.). 3,3′-Dipropylthiadicarbocyanine-iodide (DiSC3-(5)) and Calcein were purchased from Molecular Probes (Junction City, OR). All other reagents were of analytical grade. Buffers were prepared in double distilled water. Amphotericin B and trypsin (bovine pancreas) were purchased from Sigma. RPMI 1640 was purchased from Biological Industries (Beit Haemek, Israel). Proteinase K (fungal) was purchased from Beckman (Germany).

Peptide Synthesis, Acylation, and Purification. Peptides were synthesized by an F-moc solid-phase method on Rink amide MBHA resin, using a ABI 433A automatic peptide synthesizer. The synthesized peptides were purified by RP-HPLC (reversed-phase high-performance liquid chromatography) on a C_{18} Bio-Rad semipreparative column (250 × 10 mm, 300 Å pore size, 5 μm particle size). The purified peptides were shown to be homogeneous (∼95%) by analytical HPLC. Electrospray mass spectroscopy was used to confirm their molecular weight. The lipophilic acid was bound to the N-terminus using the same protocol as that used to attach protected amino acid.

Antifungal and Hemolytic Activities. The antifungal activity of the peptides was examined in sterile 96-well plates (Nunc F96 microtiter plates) in a final volume of 100 μL as follows: 50 μL of a suspension containing fungi at a concentration of 2×10^3 colony-forming units (CFU)/mL in culture medium (RPMI 1640, 0.165 M MOPS (pH 7.0) with L-glutamine and without $NaHCO_3$ medium) was added to 50 μL of water containing the peptide in serial 2-fold dilutions. The fungi were incubated for 24 h for opportunistic fungi or 48−96 h for *Candida albicans* and *Cryptococcus neoformans* at 35 °C using a Binder KB115 incubator. Growth inhibition was determined by measuring the absorbance at 620 nm in a Microplate autoreader El309 (Bio-Tek Instruments, Winooski, VT). Antifungal activity is expressed as the minimal inhibitory concentration (MIC), the concentration at which 100% inhibition of growth was observed. The fungi used were *Aspergillus fumigatus* ATCC 26430, *C. albicans* ATCC 10231, and *C. neoformans* ATCC MYA-422.

Fresh hRBC with EDTA was rinsed 3 times with PBS (35 mM phosphate buffer/0.15 M NaCl (pH 7.3)) by centrifugation for 10 min at 800*g* and resuspended in PBS. Peptides dissolved in PBS were then added to 50 μL of a solution of the stock hRBC in PBS to reach a final volume of 100 μL (final erythrocyte concentration, 4% v/v). The resulting suspension was incubated with agitation for 60 min at 37 °C. The samples were then centrifuged at 800*g* for 10 min. The release of hemoglobin was monitored by measuring the absorbance of the supernatant at 540 nm. Controls for zero hemolysis (blank) and 100% hemolysis consisted of hRBC suspended in PBS and Triton 1%, respectively.

Preparation of Liposomes. Small unilamellar vesicles (SUV) were prepared by sonication as described earlier (*21*). Briefly, dry lipids were dissolved in $CHCl_3$/MeOH (2:1, v/v). The solvents were then evaporated under a stream of nitrogen and then lyophilized overnight. The lipids were resuspended in the appropriate buffer (7 mg/mL) with vortexing, and the resulting lipid dispersions were sonicated (10−30 min) in a bath-type sonicator (G1125SP1 sonicator; Laboratory Supplies Company Inc., Hicksville, NY) until the turbidity had cleared. The vesicles were visualized using a JEOL JEM 100B electron microscope (Japan Electron Optics Laboratory Co., Tokyo, Japan). Lipid films were prepared from a mixture of zwitterionic phospholipids and ergosterol (PC/PE/PI/ergosterol, 5/2.5/2.5/1, w/w), a lipid composition used to mimic the major components of the outer leaflet of *C. albicans* (*22*).

Circular Dichroism (CD) Spectroscopy. The CD spectra of the peptides were measured with a Aviv 202 spectropolarimeter. The spectra were scanned with a thermostatic quartz optical cell with a path length of 1 mm. Each spectrum was recorded in an average time of 15 s at a wavelength range of 260−195 nm. The peptides were scanned at a concentration of 2−100 μM in PBS (35 mM phosphate buffer, 0.15 M NaCl (pH 7.3)) and 20 μM in the presence

[1] Abbreviations: ATR-FTIR, attenuated total reflectance Fourier transform infrared; CD, circular dichroism; CFU, colony-forming units; hRBC, human red blood cells; PBS, phosphate buffered saline; PI, phosphatidylinositol; PE, phosphatidylethanolamine; RP-HPLC, reversed-phase high-performance liquid chromatography.

of 8 mM palmitoyloleoylphosphocholine (POPC) vesicles. Fractional helicities (*23*, *24*) were calculated as follows:

$$\frac{[\theta]_{222} - [\theta]_{222}{}^{0}}{[\theta]_{222}{}^{100} - [\theta]_{222}{}^{0}}$$

where $[\theta]_{222}$ is the experimentally observed mean residue ellipticity at 222 nm and values for $[\theta]_{222}{}^{0}$ and $[\theta]_{222}{}^{100}$, corresponding to 0% and 100% helix content at 222 nm, are estimated to be −2000 and −32 000 (deg·cm^2)/dmol, respectively (*23*).

Analytical Ultracentrifugation. Sedimentation experiments were carried out using a Beckman Optima XL-A absorbance analytical ultracentrifuge. Peptide was dissolved in PBS at different concentrations and loaded into equilibrium six-channel, quartz-window, analytical ultracenrifugation cells. This required 110 μL of solution. The buffer (10 μL more than the total volume in the sample compartment) was loaded into each solvent compartment. Solutions were centrifuged at 3000 rpm to determine the absorbance (at 215, 229, and 280 nm) at each particular loading concentration. The absorption was constant across the cell at low speed (before detectable sedimentation occurred). Peptide was centrifuged at 48 000 rpm and 25 °C, then diluted to three concentrations (10, 20, and 50 μM) with PBS, which also filled the reference channels. The specific volume of the peptide was estimated from its amino acid sequence by the method of Cohn and Edsall (*25*), 0.7413 mL/g. The solvent density was estimated to be 1 g/mL. The data set at a given concentration was fitted with a nonlinear least-squares program for the models ideal-dilute single species and a monomer−dimer. The molar mass of the monomer was constrained to the expected value, 2742 Da.

Calcein Release Assay. Membrane permeation was assessed utilizing the calcein release assay (*26*), as previously described (*27*). Briefly, PC/PE/PI/ergosterol SUV (7 mg/mL) were prepared in a 60 mM calcein and 10 mM Tris solution (pH 7.4). Liposomes were then passed through a Sephadex G-50 column (Pharmacia Uppsala, Sweden) to separate the free calcein. A final concentration of 2.5 μM SUV was used. Trapped inside the vesicles, the calcein dye is self-quenched. Membrane permeation was detected by an increase in fluorescence, following the addition of peptide. The percentage of fluorescence recovery, F_t, was defined as

$$F_t = (I_t - I_0/I_f - I_0) \times 100$$

where I_0 = the initial fluorescence, I_f = the total fluorescence observed after maximum calcein release was achieved, and I_t = the fluorescence observed at equilibrium after adding the peptide.

In Vivo Transmembrane Potential Depolarization Assay. A potential depolarization assay was performed with fungi and yeast that were not treated with agents known to increase cell wall permeability. Membrane destabilization, which results in the collapse of transmembrane potential, was detected fluorimetrically using a fluorescence dye (*28*). The dye binds the plasma membrane because of the cell transmembrane potential, resulting in a quenching of the dye's fluorescence. Peptide-induced membrane permeation caused a dissipation of the transmembrane potential that was monitored by an increase in fluorescence due to the release of the dye. More specifically, cells were centrifuged at 4000*g* for 5 min at 4 °C in a SS-34 rotor after being incubated at 35 °C with agitation for 24 h in RPMI buffer (RPMI 1640, 0.165 M MOPS (pH 7.0) with L-glutamine and without $NaHCO_3$). The cells were resuspended in PBS (without Ca^{2+} and Mg^{2+}) to an inoculum of 4×10^3 CFU/mL. Cells were incubated with 1 μM diS−C_3-5 followed by fluorescence dequenching until a stable baseline was achieved (∼50 min), indicating the incorporation of the dye onto the yeast membrane. Experiments were performed in sterile 96-well plates (Nunc F96 microtiter plates) in a final volume of 100 μL as follows. Fifty microliters of a suspension containing yeast and the dye was added to 50 μL of water containing the peptide in serial 2-fold dilutions. Membrane depolarization was monitored by an increase in the fluorescence of diS−C_3-5 (excitation wavelength λ_{ex} = 622 nm, emission wavelength λ_{em} = 670 nm) after addition of peptides at different concentrations.

ATR-FTIR Spectroscopy. Spectra were obtained with a Bruker equinox 55 FTIR spectrometer equipped with a deuterated triglyceride sulfate (DTGS) detector and coupled with an ATR device. For each spectrum, 150 scans were collected with a resolution of 4 cm^{-1}. Samples were prepared as previously described (*29*). Briefly, lipids alone or with peptide were deposited on a ZnSe horizontal ATR prism (80 × 7 mm). Previous to samples preparations, the trifluoroacetate (CF_3COO^-) counterions, which strongly associate to the peptide, were replaced with chloride ions through several washings in 0.1 M HCl and lyophilization. This eliminated the strong C═O stretching absorption band near 1673 cm^{-1}(*30*). Peptides were dissolved in MeOH and lipids in a 1:2 MeOH/$CHCl_3$ mixture. Lipid−peptide mixtures or lipids with the corresponding volume of methanol were spread with a Teflon bar on the ZnSe prism. The solvents were eliminated by drying under vacuum for 30 min. Pure phospholipid spectra were subtracted to yield the difference spectra. The background for each spectrum was a clean ZnSe prism. The sample was hydrated by introducing an excess of deuterium oxide (D_2O) into a chamber placed on top the ZnSe prism in the ATR casting and incubating for 4 min before acquiring the spectra. H/D exchange was considered complete due to the complete shift of the amide II band. Any contribution of D_2O vapor to the absorbance spectra near the amide I peak region was eliminated by subtraction of the spectra of pure lipids equilibrated with D_2O under the same conditions.

ATR-FTIR Data Analysis. To resolve overlapping bands, we processed spectra using PEAKFIT (Jandel Scientific, San Rafael, CA) software. Second-derivative spectra were calculated to identify the positions of the component bands in the spectra. These wavenumbers were used as initial parameters for curve fitting with Gaussian component peaks. Positions, bandwidths, and amplitudes of the peaks were varied until a good agreement between the calculated sum of all components and the experimental spectra was achieved ($r^2 > 0.999$). The relative amounts of different secondary structure elements were estimated by dividing the areas of individual peaks assigned to a particular secondary structure by the whole area of the resulting amide I band.

Analysis of the Polarized ATR-FTIR Spectra. The ATR electric fields of incident light were calculated as follows (*31*, *32*):

$$E_x = \frac{2\cos\theta\sqrt{(\sin^2\theta - {n_{21}}^2)}}{\sqrt{\{(1-{n_{21}}^2)[(1+{n_{21}}^2)\sin^2\theta - {n_{21}}^2]\}}}$$

$$E_y = \frac{2\cos\theta}{\sqrt{(1-{n_{21}}^2)}}$$

$$E_z = \frac{2\sin\theta\cos\theta}{\sqrt{\{(1-{n_{21}}^2)([1+{n_{21}}^2)\sin^2\theta - {n_{21}}^2]\}}}$$

where θ is the angle of a light beam to the prism normal at the point of reflection (45°) and $n_{21} = n_2/n_1$ (n_1 and n_2 are the refractive indices of ZnSe, taken as 2.4, and of the membrane sample, taken as 1.5, respectively). Under these conditions, E_x, E_y, and E_z are 1.09, 1.81, and 2.32, respectively. The electric field components, together with the dichroic ratio (defined as the ratio between absorption of parallel (to a membrane plane), A_p, and perpendicularly polarized incident light, A_s) are used to calculate the orientation order parameter, f, by the following formula:

$$f = \frac{2({E_x}^2 - R^{ATR}{E_y}^2 + {E_z}^2)}{h(3\cos^2\alpha - 1)({E_x}^2 - R^{ATR}{E_y}^2 - 2{E_z}^2)}$$

where α is the angle between the transition moment of the amide I vibration of an α helix and the helix axis. Several values ranging from 27−40° were reported in the literature for α (*33*). We used the values of 27° (*31*, *34*) and 39° (*35*) for α. Lipid order parameters were obtained from the symmetric (∼2853 cm^{-1}) and antisymmetric (∼2922 cm^{-1}) lipid stretching modes using the same equations, setting $\alpha = 90°$ (*31*).

Tryptophan Fluorescence Measurements. To determine the environment of the peptides, changes in the intrinsic tryptophan fluorescence were measured in PBS and upon binding to vesicles. Peptide (1 μM) was added to PBS, or PBS containing 1 mM PC/PE/PI/ergosterol (5/2.5/2.5/1) SUVs. Emission spectra were measured on a SLM-Aminco, series 2 spectrofluorimeter with excitation set at 280 nm using a 4 nm slit and recorded in the range of 300−400 nm (4 nm slit). In these studies, SUV were used to minimize differential light-scattering effects, (*36*) and the lipid/peptide molar ratio was kept high (1000:1) so that spectral contributions of free peptide would be negligible.

Enzymatic Cleavage of the Lipopeptides in Aqueous Solution. Proteinase K or trypsin were added to water-dissolved magainin−HA magainin−UA and magainin−PA (1:10, w/w) and incubated for 2−4 h at room temperature. Proteolysis was assessed by RP-HPLC on a C_{18} Bio-Rad analytical column (250 × 4 mm, 300 Å pore size, 7 μm particle size) using a gradient of 10−90% acetonitrile in water (both containing 5% TFA) in 50 min.

RESULTS

Peptides Design and Sequences. We synthesized a magainin-2 analogue, in which Phe12 was substituted for tryptophan. Tryptophan served as an intrinsic fluorescent probe. Functional and structural studies revealed that the Phe12−Trp substitution did not change the properties of the parent peptide (*37*, *38*). The sequence of this analogous of magainin is G I G K F L H S A K K W G K A F V G E I M N S−NH_2.

Table 1: Minimal Inhibitory Concentration (μM) of Magainin and Lipopeptide-Conjugated Magainin[a]

	minimal inhibitory concentration (μM)		
	yeast		fungi
peptide designation	*Candida albicans* (ATCC 10231)	*Cryptococcus neoformans* (ATCC MYA-422)	*Aspergillus fomigatus* (ATCC 26430)
magainin-2	>50	25	>50
magainin−HA	50	6.25	50
magainin−UA	25	3.125	6.25
magainin−PA	>50	1.56	>50

[a] The results are the mean of three independent experiments, each performed in duplicate, with a standard deviation of 25%.

Lipophilic acid-conjugated magainin analogues were synthesized by attaching heptanoic acid (HA) ($CH_3-(CH_2)_5-$COOH), undecanoic acid (UA) ($CH_3-(CH_2)_9-$COOH), and palmitic acid (PA) ($CH_3-(CH_2)_{14}-$COOH) to the N-terminus of magainin.

Antifungal and Hemolytic Activity of the Peptides. Antifungal activity was assayed against representative pathogenic fungi that mostly infect immuno-compromised individuals (Table 1). The antifungal drug Amphotericin B served as a control and gave the reported MIC values. MIC values of the peptides on *C. albicans*, *C. neoformans*, and *A. fumigatus* are shown in Table 1. The results show a direct correlation, for the three lipopeptides tested between the length of the lipophilic acid and antifungal activity only on the sensitive yeast *C. neoformans*. However, only magainin−UA showed high potency against all species tested.

The peptides were also tested for their hemolytic activity against the highly sensitive human erythrocytes (4% solution) (data not shown). The results reveal that magainin and magainin−HA are not hemolytic at their MIC, whereas magainin−PA and magainin−UA are only slightly active.

Peptide-Induced Membrane Destabilization. To determine whether biological activity depends only on the ability of the lipopeptides to permeate target membranes, a calcein leakage assay was performed. Briefly, the peptides were mixed at various concentrations with PC/PE/PI/ergosterol SUVs (representing the outer leaflet of yeast membrane) (*22*) encapsulated with calcein. The kinetics of membrane disruption by the peptides was measured by monitoring fluorescence increases over time. The maximum calcein release level as a function of the lipid/peptide molar ratio was also determined (Figure 1). Magainin−PA and magainin−UA similarly permeate PC/PE/PI/ergosterol membranes with high potency. Magainin−HA had a lower activity and magainin had no activity within the tested range of peptide/lipid molar ratios. The correlation between membrane permeation and function can explain the biological activity of magainin, magainin−HA, and magainin−UA but not magainin−PA, which is active only toward the highly sensitive *C. neoformans*. This indicates that factors other than lipophilic tail length and direct peptide−lipid interactions are involved in peptide antifungal activity. This will be discussed in the following paragraphs.

Transmembrane Potential Depolarization of C. neoformans. To test whether the activity of magainin−PA on *C.*

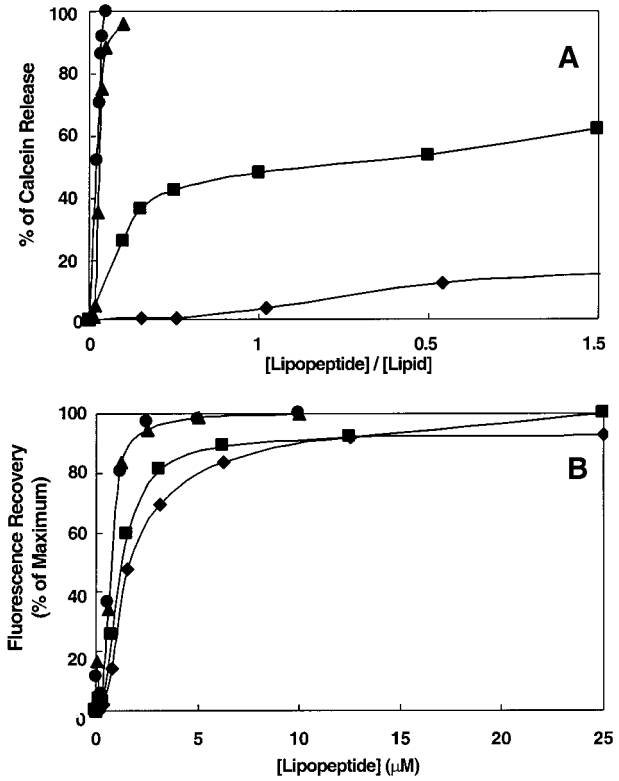

FIGURE 1: (A) Peptide-induced calcein release. Peptides were added to PC/PE/PI/ergosterol (5/2.5/2.5/1) SUV encapsulated with calcein. The increase in the fluorescence versus molar ratio of peptide/lipid was recorded: (♦) magainin, (■) magainin−HA, (▲) magainin−UA, (●) magainin−PA. (B) Depolarization of membrane potential of *C. neoformans*. Membrane destabilization, which results in the collapse of a transmembrane potential, was detected fluorimetrically using a fluorescence dye. Fifty microliters of a suspension containing *C. neoformans* and the dye were added to 50 μL of water containing the peptide in serial 2-fold dilutions. Membrane depolarization was monitored by an increase in the fluorescence of diS−C_3-5 (excitation wavelength λ_{ex} = 622 nm, emission wavelength λ_{em} = 670 nm) after the addition of peptides at different concentrations.

neoformans results from its ability to penetrate through the cell wall, we used an in vivo potential depolarization assay similar to what has been described for a permeable mutant of *Escherichia coli* (*39*). We found that magainin−PA and the dye were able to penetrate through the cell wall of only *C. neoformans* (without treatment of the yeast cell wall) but not other fungi or yeast tested. This indicates that the *C. neoformans* cell wall, unlike that of the other yeast or fungi we tested, is highly permeable. All of the tested peptides were able to dissipate the membrane potential of *C. neoformans* to a high extent (Figure 1B). Interestingly, these results correlate well with the antifungal activity of the different peptides against *C. neoformans*. Furthermore, there is good agreement between MIC and the concentration of peptide required to dissipate 100% of the yeast transmembrane potential. The slight difference might be due to the difference between the conditions used in the antifungal assay (done in RPMI buffer) and the potential depolarization assay. Furthermore, whereas the antifungal assays proceeded for 72 h at 35 °C, the dissipation of the membrane potential was performed for up to 50 min at 25 °C. Overall, the findings that all of the peptides have a similar potency in increasing the permeability of PC/PE/PI/ergosterol membranes, together (Figure 1A) with the finding of a direct correlation between MIC of the peptides and their ability to dissipate the yeast membrane potential, suggests that the difference in their activities results from differences in their ability to reach the inner membrane.

Table 2: Tryptophan Emission Maxima (in nm) of the Peptides in Solution or in the Presence of PC/PE/PI/Ergosterol (5/2.5/2.5/1, w/w) Vesicles

peptide designation	PBS	membrane[a]
magainin	351 ± 1	340 ± 1
magainin−HA	351 ± 1	337 ± 2
magainin−UA	350 ± 1	336 ± 1
magainin−PA	339 ± 1	337 ± 1

[a] A lipid-to-peptide molar ratio of 1000:1 was used in all cases.

Localization of the Tryptophan Environment Upon Transfer From Solution to Membranes. We monitored the fluorescence emission spectrum of the tryptophan (*40*, *41*) in PBS and in the presence of PC/PE/PI/ergosterol vesicles (5/2.5/2.5/1, w/w). The emission of tryptophan is affected by the polarity of the environment. As the polarity decreases, the intensity of the emission increases, and a blueshift is observed. SUV were used to minimize light-scattering effects, (*36*) and a high lipid/peptide molar ratio was maintained (1000:1) so that spectral contributions of free peptide would be negligible. The results are summarized in Table 2. In buffer, the emission maximum of tryptophan revealed a hydrophilic environment only for magainin, magainin−HA, and magainin−UA. When PC/PE/PI/ergosterol vesicles were added to the aqueous solutions containing these peptides, similar blueshifts were observed for all peptides, reflecting relocation to a more hydrophobic environment (*42*). In contrast, the emission maximum of the tryptophan in magainin−PA showed a blueshift (337 ± 1 nm) in aqueous solution, indicating a hydrophobic environment. Upon membrane binding, no significant blueshift was observed, indicating that tryptophan is located in a similar hydrophobic environment in both cases. A possible explanation for this observation will be given in the following sections. A decrease in emission intensity was observed for all the peptides upon binding to the membrane, suggesting fluorescence quenching due to peptide assembly within the membrane (data not shown).

Oligomeric State of the Peptides in Solution Determined by Tryptophan Fluorescence. The effect of increasing peptide concentration on the maximum of tryptophan emission was used as an indicator of peptide oligomeric state in solution. Increasing concentrations of the peptides from 1 to 90 μM were added to PBS, and tryptophan fluorescence was monitored. No changes were observed with magainin (351 ± 1 nm), magainin−HA (351 ± 1 nm), and magainin−PA (339 ± 1 nm). With magainin−UA, a dose-dependent blueshift in the emission maximum of the tryptophan and an increase in fluorescence were observed from 350 ± 1 nm at 1 μM to 343 ± 1 nm at 90 μM, the maximum concentration tested (Figure 2). These results suggest oligomerization of magainin−UA in aqueous solution (*43*, *44*). Oligomerization results in the lipophilic acid having a hydrophobic environment, probably due to its micellization.

Oligomeric State of the Peptides in Solution Determined by CD Spectroscopy. The effect of the lipophilic acid moiety on the extent of magainin α-helical structure in PBS was determined from the CD spectra of the lipopeptides. CD

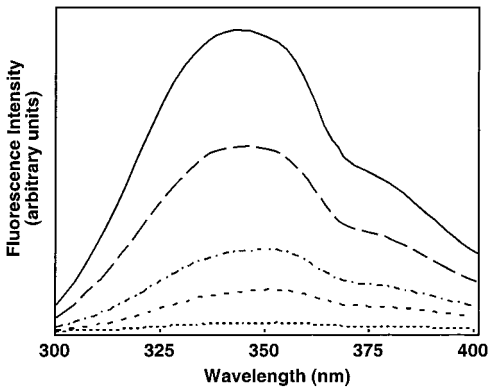

FIGURE 2: Aggregation of magainin−UA in aqueous solution. The aggregation state of magainin−UA was detected by following intrinsic tryptophan fluorescence maxima in PBS (35 mM phosphate buffer/0.15 M NaCl (pH 7.4) at 24 °C). Excitation was set at 280 nm and emission was recorded in the range of 300−400 nm. Peptide concentrations from the lower to the upper curves are 1, 10, 22, 47, and 90 μM.

spectral profiles of the peptides at different concentrations (from 2 to 100 μM) in PBS are shown in Figure 3. Interestingly, magainin−PA adopted 55% α helix at all concentrations tested, indicating that the peptide has an intrinsic, stable α-helical conformation. In contrast, magainin−UA showed concentration-dependent α-helical structure, indicating that the formation of aggregates or micelles affected the secondary structure. Up to 100 μM, both magainin and magainin−HA showed spectra characteristic of random coils. Similar results were reported for native magainin-2 using FTIR (*20*). Our results indicated that heptanoic acid is too short to stabilize an amphipatic α-helical structure in solution at the concentrations tested.

Oligomeric State of Magainin−PA in Aqueous Solution, As Determined by Analytical Ultracenrifugation. Because magainin−PA adopts a highly helical structure in solution, independent of its concentration, it was of great importance to find out whether it forms an oligomer composed of a fixed number of monomers or it exists as a monomer. The oligomeric state of magainin−PA in aqueous solution was therefore determined using analytical ultracentrifugation. Briefly, the peptide was dissolved in PBS at three different concentrations: 10, 20, and 50 μM. Centrifugation for ∼24 h at 30 000 rpm failed to sediment magainin−PA. After increasing the speed to 45 000 rpm overnight, equilibrium was reached. The data were best fit to a monomer, with a small dimer population (Figure 4). Note that the partial specific volume of the lipopeptide was calculated according to its amino acid sequence without considering the lipid moiety. Addition of the lipid to this calculation may increase its value. Using a higher value for the specific volume results in a negligible dimer population, indicating that up to 50 μM of the lipopeptide is monomeric in aqueous solution.

Secondary Structure of the Peptides in Membranes Determined by ATR-FTIR and CD Spectroscopy. We used both ATR-FTIR and CD spectroscopy to determine the secondary structure of magainin and its lipophilic acid conjugates in SUV. In FTIR spectroscopy, helical and unordered structures can contribute to the amide I vibration at almost identical wavenumbers, and it is therefore difficult to determine the precise proportion of helix and random coil from the IR spectra. However, the exchange of hydrogen with deuterium sometimes makes it possible to differentiate α-helical components from random structure, because the random structure absorption shifts to a higher extent than the α-helical component after deuteration. Therefore, we examined the IR spectra of the peptides after complete deuteration. PC/PE/PI/ergosterol was used at a lipid−peptide molar ratio of 60:1. Examples of the amide I region spectra of magainin

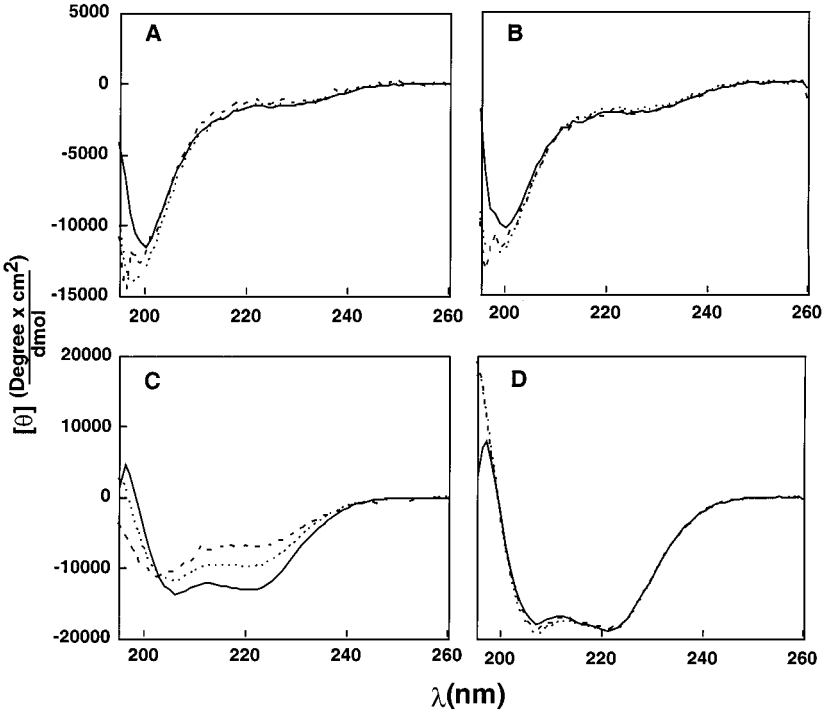

FIGURE 3: CD spectra of the peptides in PBS. Spectra were taken at peptide concentrations ranging from 20 to 100 μM. The assay was performed as described in the Materials and Methods section: (---) 20 μM, (•••) 50 μM, (—) 100 μM; panel A, magainin; panel B, magainin−HA; panel C, magainin−UA; panel D, magainin−PA.

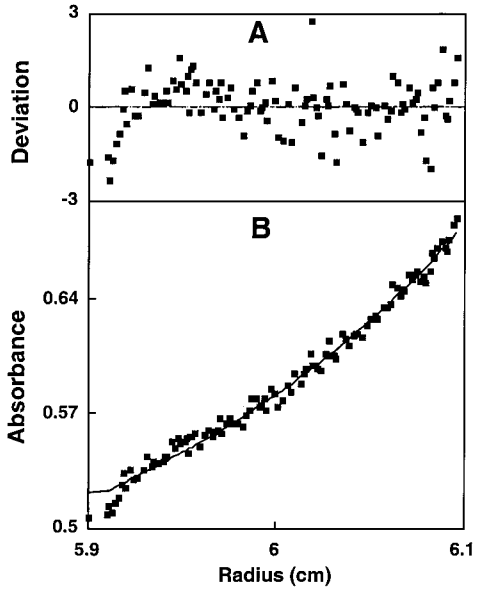

FIGURE 4: Sedimentation equilibrium experiment for magainin−PA in PBS. Experimental conditions: temperature, 25 °C; rotor speed, 45 000 rpm; loading concentration, 10 μM. The data best fitted the monomer model.

and magainin lipopeptides bound to PC/PE/PI/ergosterol (5/2.5/2.5/1, w/w) multibilayers are shown in Figure 5. Second derivatives with 15% Savitsky−Golay smoothing were calculated to identify the positions of the component bands in the spectra and are given in the corresponding panels in Figure 5. These wavenumbers were used as initial parameters for curve fitting with Gaussian component peaks. The assignments, wavenumbers (υ), and relative areas of the component peaks are summarized in Table 3. Assignment of the different secondary structures to the various amide I regions was calculated according to the values taken from Jackson and Mantsch (*45*). The amide I region from 1625 to 1640 cm^{-1} is characteristic of a β-sheet structure, whereas the amide I region of an α-helical structure is located between 1650 and 1655 cm^{-1} (*46*). All of the peptides adopt similar structures of ∼60% α helix (∼1655 ± 1 cm^{-1}) and ∼35% β sheet (∼1635 ± 1 cm^{-1}). The assignment of the component at ∼1655 ± 1 cm^{-1} to an α-helical structure is further supported by two-dimensional ^{1}H NMR of native magainin-2 in a hydrophobic environment (*47*, *48*).

The secondary structures in membranes obtained by using ATR-FTIR spectroscopy are similar to those obtained by using CD spectroscopy in POPC vesicles (spectra not shown). Magainin, magainin−HA, magainin−UA, and magainin−PA adopt 52%, 70%, 65%, and 58% α-helical structures, respectively.

Orientation of the Peptides in Lipid Multibilayers Determined by ATR-FTIR Spectroscopy. Polarized ATR-FTIR was used to determine the orientation of the peptides within lipid bilayers. The order parameter of the helical portion of magainin and magainin's lipopeptides, *f*, was calculated from the ATR−dichroic ratio of the amide I band. The dichroic ratio values, *R*, were calculated from the amide I absorption at ∼1655 cm^{-1} (the major component of the amide I band, as revealed by the second derivative) in the polarized spectra. The corresponding order parameters, assuming $\alpha = 27°$ (*31*, *34*) or $\alpha = 39°$ (*35*), were calculated as described in Materials and Methods and are summarized in Table 4.

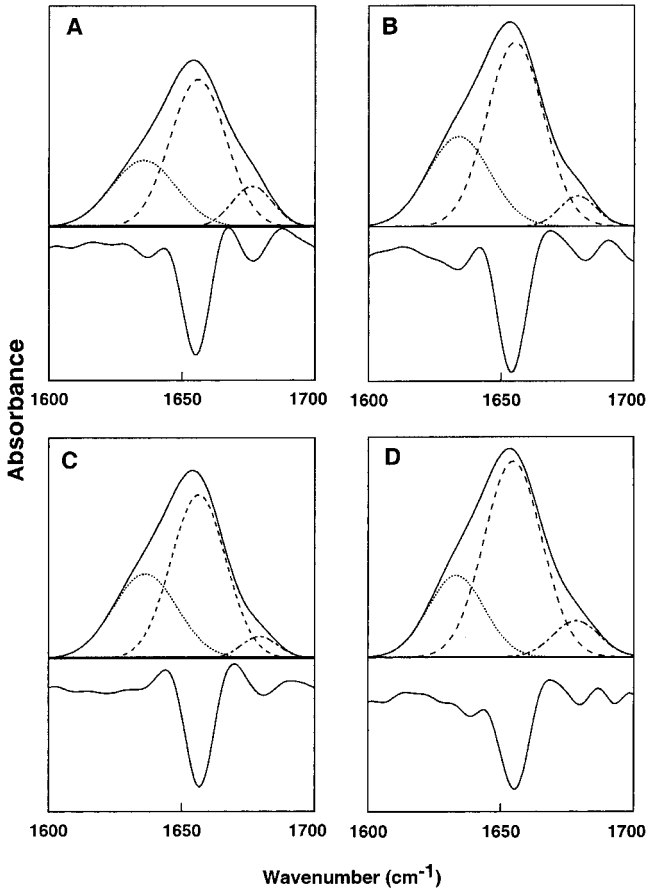

FIGURE 5: FTIR spectral deconvolution of the fully deuterated amide I band (1600−1700 cm^{-1}) (upper spectrum in each panel) and second derivatives (lower spectrum in each panel) of magainin (panel A), magainin−HA (panel B), magainin−UA (panel C), and magainin−PA (panel D) in PC/PE/PI/ergosterol (5/2.5/2.5/1) multibilayers. The second derivatives were calculated to identify the positions of the component bands in the spectra. The component peaks are the result of curve fitting using a Gaussian line shape. The amide I frequencies, characteristic of the various secondary structure elements, were taken from Jackson and Mantsch (*45*). The sums of the fitted components are superimposed on the experimental amide I region spectra. In the upper spectra on the panels, the continuous lines represent the experimental FTIR spectra after Savitzky−Golay smoothing; the broken lines represent the fitted components. A 60:1 lipid/peptide molar ratio was used.

Negative order parameters were observed for all peptides, typical of helices oriented nearly parallel to the membrane surface (*33*). This indicates that the orientation of the peptide within the lipopeptide is not affected by the attachment of the lipophilic acid and is similar to the orientation of the parental peptide.

Orientation of the Phospholipid Membrane and the Effect of the Peptides on Phospholipid Acyl-Chain Order. Polarized ATR-FTIR spectroscopy was used to determine the orientation of the lipid membrane. The symmetric [$\upsilon_{sym}(CH_2) \approx$ 2853 cm^{-1}] and the antisymmetric [$\upsilon_{sym}(CH_2) \approx$ 2922 cm^{-1}] vibrations of lipid methylene C−H bonds are perpendicular to the molecular axis of a fully extended hydrocarbon chain. Thus, measurements of the dichroism of infrared light absorbance can reveal the order and orientation of the membrane sample relative to the prism surface. However, because the intensity of the antisymmetric CH_2 vibration was higher than 1, our calculations were based only on *R* values taken from the symmetric vibration. On the basis of the

Table 3: Assignment, Wavenumbers (υ), and Relative Areas of the Component Peaks Determined from the Deconvolution of the Amide I Bands of the Peptides Incorporated into PC/PE/PI/ergosterol (5/2.5/2.5, w/w) Multibilayers[a,b]

	secondary structure					
	β sheet		α helix		high-frequency β sheet/turn	
peptide designation	υ (cm^{-1})	area (%)	υ (cm^{-1})	area (%)	υ (cm^{-1})	area (%)
magainin-2	1635 ± 1	28 ± 2	1656 ± 1	56 ± 2	1675 ± 1	16 ± 4
magainin−HA	1634 ± 1	30 ± 3	1655 ± 1	63 ± 2	1678 ± 1	7 ± 1
magainin−UA	1636 ± 1	36 ± 4	1656 ± 1	58 ± 4	1679 ± 1	6 ± 2
magainin−PA	1635 ± 2	24 ± 2	1654 ± 1	65 ± 1	1677 ± 1	11 ± 1

[a] A 1: 60 peptide: lipid molar ratio was used. All values are given as mean ± standard deviation. [b] The results are the average of four independent experiments.

Table 4: ATR−FTIR Dichroic Analysis

	membrane[a] order[b]		peptide orientation		
peptide designation	R of υ_{sym}	f of υ_{sym}	R	$f_{\alpha = 27°}$	$f_{\alpha = 39°}$
membrane[a]	1.42 ± 0.01	0.27 ± 0.01			
membrane[a] + magainin	1.56 ± 0.02	0.20 ± 0.01	1.86 ± 0.05	−0.04 ± 0.01	−0.05 ± 0.02
membrane[a] + magainin−HA	1.55 ± 0.01	0.21 ± 0.03	1.71 ± 0.04	−0.07 ± 0.01	−0.10 ± 0.01
membrane[a] + magainin−UA	1.52 ± 0.03	0.22 ± 0.02	1.67 ± 0.01	−0.083 ± 0.002	−0.12 ± 0.03
membrane[a] + magainin−PA	1.56 ± 0.02	0.20 ± 0.01	1.71 ± 0.01	−0.074 ± 0.004	−0.09 ± 0.02

[a] Phospholipid membrane of PC/PE/PI/ergosterol (5/2.5/2.5/1) was used. [b] A 1:60 peptide/lipid molar ratio was used.

dichroic ratio of lipid stretching, the corresponding order parameter, *f*, was calculated and is summarized in Table 4. Antisymmetric (~2922 cm^{-1}) and symmetric peaks (~2853 cm^{-1}) indicate that the membranes are predominantly in a liquid-crystalline phase (*31*, *49*). Thus, the lipid multibilayers used in the study were well-oriented and in a liquid-crystalline phase. The effect of the peptides on the multibilayer acyl-chain orders can be estimated by comparing the CH_2− stretching dichroic ratio of pure phospholipid multibilayers and membrane-bound peptides. The data indicate that incorporation of the peptides into the membrane did not significantly change the lipid order (see Table 4), suggesting that all of the peptides are surface-localized and do not significantly destabilize the acyl-chain order. Interestingly, both magainin and lipo−magainin disrupt the acyl-chain order to the same extent, suggesting that attachment did not alter magainin−membrane interaction.

Proteolytic Enzymes Treatment of the Lipopeptides. Treatment of magainin−HA and magainin−UA with the proteolytic enzymes Proteinase K or trypsin resulted in a complete digestion of the peptides. In contrast, treatment of magainin−PA with the two enzymes revealed 100% or 70% resistance to proteolysis, respectively, after 4 h of treatment (the maximum time tested) (data not shown). This can be explained by the unique, stable, and concentration-independent structure of magainin−PA in aqueous solution, which apparently hides the cleavage sites of the peptide from the enzymes. On the other hand, in the case of magainin−UA, full digestion indicates that the peptide backbone is exposed to the aqueous environment.

DISCUSSION

Lipophilic Acid Effects on Peptide Structure, Oligomeric State in Solution, and Stability to Proteolysis. Magainin and magainin−HA form monomeric random coils in buffer, similar to what has been reported previously for magainin (*20*). In contrast, the more hydrophobic magainin−UA and magainin−PA adopt α-helical structures in PBS (Figure 3).

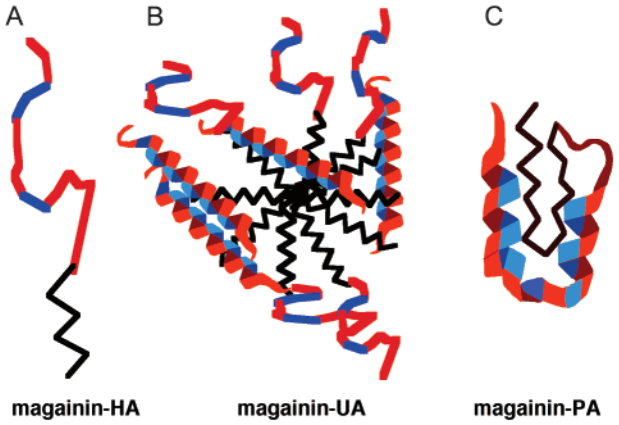

FIGURE 6: Cartoon illustrating possible organizations of the three lipopeptides studied. Red represents hydrophilic amino acids, and blue represents hydrophobic amino acids.

This suggests a threshold of hydrophobicity above heptanoic acid is required to form a sufficiently hydrophobic environment to stabilize an α-helical conformation for magainin in aqueous solution. The simplest way to envision the formation of a hydrophobic environment by lipophilic acids is through self-association to form micelles. In addition, the tendency to oligomerize is offset by the resulting close apposition of positively charged magainin monomers. Hydrophobic interactions between the short heptanoic acyl chains might not be sufficient to overcome the electrostatic repulsions between the positive charges of magainin monomers in aqueous solution to form micelles. The inability to detect a change in the tryptophan fluorescence signal also supports this conclusion. Aggregation constitutes the preferred organization of α helices with their hydrophobic surfaces facing each other. In this scenario, lipopeptides would form concentration-dependent oligomers, as seen in magainin−UA (Figure 2). One such possible oligomer is envisioned in Figure 6B. The most hydrophobic lipopeptide, magainin−PA, adopts a stable α-helical structure that is concentration-independent. This stable α-helical conformation has been confirmed by

analytical ultracentrifugation to be a monomer, not the oligomer (Figure 4) expected if miscellization occurs. To our knowledge, this is the first report of an amphipathic α-helical structure stabilized by a single lipophilic hydrocarbon chain. The PA acyl chain is long enough to interact with the peptide's hydrophobic side chain. To minimize exposure of methylene groups to the polar solvent, the acyl chain could bend over itself. In parallel, the peptide moiety covers the acyl chain's outer surface by forming an amphipatic α helix with its hydrophobic surface toward the lipid chain. The hydrophilic surface is exposed and makes the molecule highly soluble in water (Figure 6C). In this way, the stable monomeric helical structure is not dependent on magainin−PA concentration. This model also explains why tryptophan emission indicates a hydrophobic environment at a very low concentration of the peptide (1 μM). It has been shown, in the case of chemical surfactants, that the longer the lipophilic acyl chain, the more effective is micellization, because of an increase in intermolecular hydrophobic interactions (*50*). According to our results, however, micelles formation can be abolished if the lipophilic acyl chain is long enough to interact with the peptide moiety covalently bound to it. These significant differences in structure and oligomeric state between magainin−UA and magainin−PA in solution probably are the major factor underlying the differences in their antifungal activities against *C. albicans* and *A. fumigatus*, as discussed next. These differences can also explain the high stability of magainin−PA to enzymatic degradation as compared with the other two lipopeptides.

Membrane-Bound Lipopeptides Structures and Activity. Magainin−PA and magainin−UA were either not hemolytic or showed only low hemolytic activities at their lower MIC when tested against a highly dilute solution of 4% human erythrocytes (data not shown). The ability of the lipopeptides to destabilize PC/PE/PI/ergosterol vesicles, representing the major components of the outer leaflet of pathogenic yeasts (Figure 1), correlates with the length of the attached lipophilic acid. This can be explained by increased affinity of lipopeptides to vesicles as a result of hydrophobic interactions. This is supported by earlier studies of Peitzsch and McLaughlin, showing that the binding energies of the anionic form of fatty acids and the corresponding acylated glycines or tripeptides were identical and the energies increased by 0.8 kcal/mol per number of carbons in the acyl chain (*51*). Although each lipopeptide shows a different affinity to phospholipid membranes, once bound, all three of them are oriented parallel to the membrane surface and alter the membrane order similar to the parental peptide, magainin. This can be explained by the insertion of the lipidic moiety perpendicular to the membrane surface as one of the membrane phospholipids, whereas the binding of the peptidic moiety is parallel to the membrane surface (similarly to magainin). This should result in a similar membrane order for all of them. Once the lipopeptides bind the membrane, they obtain their thermodynamically favorable conformation, an amphipathic α-helical structure, which is responsible for their membrane-permeating activity. This structure is confirmed by CD and FTIR spectroscopies and is similar for all three lipopeptides in their membrane-bound state. Accordingly, the binding energy of magainin−PA should be ∼4 kcal/mol higher than that of magainin−UA. However, they have similar membrane-permeating abilities. A possible explanation is that magainin−UA reaches the membrane already partially oligomerized, compensating over the pre-existing, α-helical structure of magainin−PA.

A good correlation was found between the activity of magainin−PA against *C. neoformans* (MIC = 1.56 μM) and its ability to dissipate transmembrane potential in both model membranes and the intact yeast. However, magainin−PA was totally inactive toward C. *albicans* and *A. fumigatus* (up to 50 μM, the maximum concentration tested). This might be explained by the inability of the peptide to cross the cell wall of these species, which is supported by our findings that the fluorescent dye could not penetrate into the plasma membrane of these species. The direct correlation between the MIC, the in vivo transmembrane potential depolarization assays with the permeable *C. neoformans* and the in vitro calcein release assay, suggests that the lipopeptides act directly on the cell plasma membrane.

The present data indicate that hydrophobicity and the ability to permeate fungal membranes are insufficient to kill fungi. To reach the target fungal phospholipid membrane, the peptide has to cross the cell wall containing, among other things, chitin, a variety of mannoproteins, and β- or α-linked glucans. Glucans and chitin are predominantly found in the inner layer, and mannoproteins are predominantly found in the outer layer of the wall (*52*).

The pre-existing α-helical structure of magainin−PA increases the volume of the molecule, and together with a positively charged hydrophilic surface, it might make it difficult for the peptide to diffuse through the cell wall, unless it is thin. It should be noted, however, that magainin−UA forms micelles, which should have a larger volume than that of magainin−PA. However, because micelles are in equilibrium with monomers, the small sized monomers probably insert through the cell wall, followed by further dissociation of the micelles.

Native lipopeptides exist that have a broad range of activities, including antibacterial, antifungal, antiviral, and cytolytic activity (*53*−*56*). They are produced, nonribosomally, in bacteria, yeast, or fungi during cultivation on various carbon sources (*57*). Unlike our designed magainin-2 analogue lipopeptides, what distinguishes most natural lytic agents are their unusually short lengths (6−7 amino acids), cyclization (*58*), negative charge, and mainly hydrophobic and acidic L- and D-amino acid compositions. These native lipopeptides have been shown to act via two different mechanisms: (i) inhibiting the synthesis of cell wall components such as (1,3)-β-D-glucan or chitin (*59*, *60*) and (ii) membrane lysis, although the details are unknown (e.g., iturins, bacillomycin, and surfactin) (*61*−*63*). Lipopeptide activity is highly sensitive to amino acid sequence and the attached lipid type, which is short and unsaturated in most native lipopeptides. The results described here with lipophilic acid conjugated magainin-2 analogue, which show activity against model membranes, suggest that their mode of action can be accounted for by membrane lysis, similar to unmodified magainin.

In summary, the attachment of heptanoic, undecanoic, and palmitic acids to a magainin-2 analogue results in three lipopeptides with distinct oligomeric states, structures, and stability to proteolysis in solution. The lipophilic group was found to be crucial but not sufficient for antifungal activity.

A direct correlation was found between oligomerization of the lipopeptides in solution and potent antifungal activity. These results provide insight to a new approach of modulating hydrophobicity and self-assembly of antimicrobial peptides in solution without altering the sequence of the peptide chain. These data pave the way to develop and design a new group of lipopeptide candidates for therapeutic use against fungal infections.

REFERENCES

1. Denning, D. W. (1991) *J. Antimicrob. Chemother. 28*, 1−16.
2. Alexander, B. D., and Perfect, J. R. (1997) *Drugs 54*, 657−678.
3. Boman, H. G. (1995) *Annu. Rev. Immunol. 13*, 61−92.
4. Hoffmann, J. A., Kafatos, F. C., Janeway, C. A., and Ezekowitz, R. A. (1999) *Science 284*, 1313−1318.
5. Lamberty, M., Ades, S., Uttenweiler-Joseph, S., Brookhart, G., Bushey, D., Hoffmann, J. A., and Bulet, P. (1999) *J. Biol. Chem. 274*, 9320−9326.
6. Meister, M., Hetru, C., and Hoffmann, J. A. (2000) *Curr. Top. Microbiol. Immunol. 248*, 17−36.
7. Oren, Z., and Shai, Y. (1998) *Biopolymers 47*, 451−463.
8. Hwang, P. M., and Vogel, H. J. (1998) *Biochem. Cell Biol. 76*, 235−246.
9. Dathe, M., and Wieprecht, T. (1999) *Biochim. Biophys. Acta 1462*, 71−87.
10. Tossi, A., Sandri, L., and Giangaspero, A. (2000) *Biopolymers 55*, 4−30.
11. Bechinger, B. (1999) *Biochim. Biophys. Acta 1462*, 157−183.
12. Blondelle, S. E., Perez-Paya, E., and Houghten, R. A. (1996) *Antimicrob. Agents Chemother. 40*, 1067−1071.
13. Wade, D., Boman, A., Wahlin, B., Drain, C. M., Andreu, D., Boman, H. G., and Merrifield, R. B. (1990) *Proc. Natl. Acad. Sci. U.S.A. 87*, 4761−4765.
14. Bessalle, R., Kapitkovsky, A., Gorea, A., Shalit, I., and Fridkin, M. (1990) *FEBS Lett. 274*, 151−155.
15. Shai, Y., and Oren, Z. (1996) *J. Biol. Chem. 271*, 7305−7308.
16. Verkleij, A. J., Zwaal, R. F., Roelofsen, B., Comfurius, P., Kastelijn, D., and Deenen, L. V. (1973) *Biochim. Biophys. Acta 323*, 178−193.
17. Strahilevitz, J., Mor, A., Nicolas, P., and Shai, Y. (1994) *Biochemistry 33*, 10951−10960.
18. Ghosh, J. K., Shaool, D., Guillaud, P., Ciceron, L., Mazier, D., Kustanovich, I., Shai, Y., and Mor, A. (1997) *J. Biol. Chem. 272*, 31609−31616.
19. Oren, Z., Lerman, J. C., Gudmundsson, G. H., Agerberth, B., and Shai, Y. (1999) *Biochem. J. 341*, 501−513.
20. Jackson, M., Mantsch, H. H., and Spencer, J. H. (1992) *Biochemistry 31*, 7289−7293.
21. Shai, Y., Bach, D., and Yanovsky, A. (1990) *J. Biol. Chem. 265*, 20202−20209.
22. Schneiter, R., Brugger, B., Sandhoff, R., Zellnig, G., Leber, A., Lampl, M., Athenstaedt, K., Hrastnik, C., Eder, S., Daum, G., Paltauf, F., Wieland, F. T., and Kohlwein, S. D. (1999) *J. Cell Biol. 146*, 741−754.
23. Wu, C. S., Ikeda, K., and Yang, J. T. (1981) *Biochemistry 20*, 566−570.
24. Greenfield, N., and Fasman, G. D. (1969) *Biochemistry 8*, 4108−4116.
25. Cohn, E. J., and Edsall, J. T. (1943) *Proteins, Amino Acids, and Peptides*, Reinhold, New York.
26. Allen, T. M., and Cleland, L. G. (1980) *Biochim. Biophys. Acta 597*, 418−426.
27. Pouny, Y., Rapaport, D., Mor, A., Nicolas, P., and Shai, Y. (1992) *Biochemistry 31*, 12416−12423.
28. Sims, P. J., Waggoner, A. S., Wang, C. H., and Hoffmann, J. R. (1974) *Biochemistry 13*, 3315−3330.
29. Gazit, E., Miller, I. R., Biggin, P. C., Sansom, M. S. P., and Shai, Y. (1996) *J. Mol. Biol. 258*, 860−870.
30. Surewicz, W. K., Mantsch, H. H., and Chapman, D. (1993) *Biochemistry 32*, 389−394.
31. Ishiguro, R., Kimura, N., and Takahashi, S. (1993) *Biochemistry 32*, 9792−9797.
32. Harrick, N. J. (1967) *Internal Reflection Spectroscopy*, Interscience, New York.
33. Tamm, L. K., and Tatulian, S. A. (1997) *Q. Rev. Biophys. 30*, 365−429.
34. Rothschild, K. J., and Clark, N. A. (1979) *Science 204*, 311−312.
35. Bradbury, E. M., Brown, L., Downie, A. R., Elliot, A., Fraser, R. D., and Hanby, W. E. (1962) *J. Mol. Biol. 5*, 230−247.
36. Mao, D., and Wallace, B. A. (1984) *Biochemistry 23*, 2667−2673.
37. Schumann, M., Dathe, M., Wieprecht, T., Beyermann, M., and Bienert, M. (1997) *Biochemistry 36*, 4345−4351.
38. Matsuzaki, K., Murase, O., Tokuda, H., Funakoshi, S., Fujii, N., and Miyajima, K. (1994) *Biochemistry 33*, 3342−3349.
39. Zhang, L., Scott, M. G., Yan, H., Mayer, L. D., and Hancock, R. E. (2000) *Biochemistry 39*, 14504−14514.
40. Vogel, H. (1981) *FEBS Lett. 134*, 37−42.
41. Dufourcq, J., and Faucon, J. F. (1977) *Biochim. Biophys. Acta 467*, 1−11.
42. Talbot, J. C., Faucon, J. F., and Dufourcq, J. (1987) *Eur. Biophys. J. 15*, 147−157.
43. Terwilliger, T. C., Weissman, L., and Eisenberg, D. (1982) *Biophys. J. 37*, 353−361.
44. van Veen, M., Georgiou, G. N., Drake, A. F., and Cherry, R. J. (1995) *Biochem. J. 305*, 785−790.
45. Jackson, M., and Mantsch, H. H. (1995) *Crit. Rev. Biochem. Mol. Biol. 30*, 95−120.
46. Tatulian, S. A., Biltonen, R. L., and Tamm, L. K. (1997) *J. Mol. Biol. 268*, 809−815.
47. Marion, D., Zasloff, M., and Bax, A. (1988) *FEBS Lett. 227*, 21−26.
48. Gesell, J., Zasloff, M., and Opella, S. J. (1997) *J. Biomol. NMR 9*, 127−135.
49. Cameron, D. G., Casal, H. L., Gudgin, E. F., and Mantsch, H. H. (1980) *Biochim. Biophys. Acta 596*, 463−467.
50. Rosen, M. J. E. (1989) *Surfactants and Interfacial Phenomena*, Wiley, New York.
51. Peitzsch, R. M., and McLaughlin, S. (1993) *Biochemistry 32*, 10436−10443.
52. Groll, A. H., De Lucca, A. J., and Walsh, T. J. (1998) *Trends Microbiol. 6*, 117−124.
53. Arima, K., Kakinuma, A., and Tamura, G. (1968) *Biochem. Biophys. Res. Commun. 31*, 488−494.
54. Bernheimer, A. W., and Avigad, L. S. (1970) *J. Gen. Microbiol. 61*, 361−369.
55. Muhlradt, P. F., Kiess, M., Meyer, H., Sussmuth, R., and Jung, G. (1997) *J. Exp. Med. 185*, 1951−1958.
56. Vollenbroich, D., Ozel, M., Vater, J., Kamp, R. M., and Pauli, G. (1997) *Biologicals 25*, 289−297.
57. Fiechter, A. (1992) *Trends Biotechnol. 10*, 208−217.
58. De Lucca, A. J., and Walsh, T. J. (1999) *Antimicrob. Agents Chemother. 43*, 1−11.
59. Balkovec, J. (1994) *Expert Opin. Invest. Drugs* 65−82.
60. Debono, M., and Gordee, R. S. (1994) *Annu. Rev. Microbiol. 48*, 471−497.
61. Maget-Dana, R., and Peypoux, F. (1994) *Toxicology 87*, 151−174.
62. Maget-Dana, R., and Ptak, M. (1995) *Biophys. J. 68*, 1937−1943.
63. Peypoux, F., Bonmatin, J. M., and Wallach, J. (1999) *Appl. Microbiol. Biotechnol. 51*, 553−563.

BI011549T